Cross-Linking between the Regulatory Regions of Troponin-I and Troponin-C Abolishes the Inhibitory Function of Troponin†

Yin Luo,‡ Bing Li,‡ Guang Yang,‡ John Gergely,‡,§,|| and Terence Tao*‡,⊥,#

Muscle and Motility Group, Boston Biomedical Research Institute, Watertown, Massachusetts 02472, Neurology Service, Massachusetts General Hospital, Boston, Massachusetts, 02114, Department of Biological Chemistry and Molecular Pharmacology, Harvard Medical School, Boston, Massachusetts 02115, Department of Neurology, Harvard Medical School, Boston, Massachusetts 02115, and Department of Biochemistry, Tufts University School of Medicine, Boston, Massachusetts 02111

Received June 3, 2002; Revised Manuscript Received August 28, 2002

ABSTRACT: We reported previously that both residues 48 and 82 on opposite sides of troponin-C's (TnC's) N-terminal regulatory hydrophobic cleft photo-cross-linked to Met121 of troponin-I (TnI) [Luo, Y., Leszyk, J., Qian, Y., Gergely, J., and Tao, T. (1999) *Biochemistry 38*, 6678−6688]. Here we report that the Ca^{2+}-absent inhibitory activity of troponin (Tn) was progressively lost as the extent of photo-cross-linking increased. To extend these studies, we constructed a mutant TnI with a single cysteine at residue 121 (TnI121). In Tn complexes containing TnI121 and mutant TnCs with a single cysteine at positions 12, 48, 82, 98, or 125 (TnC12, TnC48 etc.), TnI121 formed disulfide cross-links primarily with TnC48 and TnC82 when Ca^{2+} was present, and with only TnC48 when Ca^{2+} was absent. These results indicate that TnI Met121 is situated within the N-domain hydrophobic cleft of TnC in the presence of Ca^{2+}, and that it moves out of the cleft upon Ca^{2+} removal but remains within the vicinity of TnC. Activity assays revealed that the Met121 to Cys mutation in TnI121 reduced the Ca^{2+}-present activation of Tn, indicating that Met121 is important in hydrophobic interactions between this TnI region and TnC's N-domain cleft. The formation of a disulfide cross-link between TnI121 and TnC48 or TnC82 abolished the Ca^{2+}-absent inhibitory activity of Tn, indicating that the movement of the Met121 region of TnI out of TnC's N-domain cleft is essential for the occurrence of further events in the inhibitory process of skeletal muscle contraction. On the basis of these and other results, a simple mechanism for Ca^{2+} regulation of skeletal muscle contraction is presented and discussed.

Troponin-I (TnI)[1] is the inhibitory subunit of the heterotrimeric, Ca^{2+}-binding regulatory protein troponin (Tn) in skeletal and cardiac muscle. The other two subunits are troponin-C (TnC), the Ca^{2+}-binding subunit, and troponin-T (TnT), the tropomyosin (Tm)-binding subunit. Together with Tm, Tn regulates the contraction of striated muscle in a Ca^{2+}-dependent manner, relaxed (inhibited) in the absence of Ca^{2+} and contracting (activated) in its presence [reviewed recently by Gordon et al. (*1*)]. Early biochemical studies on TnC [reviewed previously in refs *2*−*4*] and its crystal structure (*5*−*8*) reveal that it is composed of an N- and a C-domain linked by a single α-helix, each domain containing two E−F hand motifs and two metal ion binding sites. The C-domain sites (III and IV) bind Ca^{2+} with high affinity, and also Mg^{2+} with lower affinity. The N-domain sites (I and II) are specific for Ca^{2+} and had been identified as the physiologically relevant regulatory sites (*9*, *10*). The crystal structures also reveal two hydrophobic clefts, one in each domain. In the structure with two Ca^{2+} ions bound at the C-domain sites ($2Ca^{2+}$•TnC), the C-domain cleft is open, while the N-domain cleft is closed (*5*, *7*). In the structure with both the C- and N-domain metal-binding sites occupied, both hydrophobic clefts are open (*6*, *8*). No other significant difference in conformation between these two structures was observed. Under physiological conditions the C-domain sites are always occupied by either Ca^{2+} or Mg^{2+}, while the N-domain sites can be expected to be unoccupied or occupied by Ca^{2+} in the relaxed or contracting conditions, respectively. This implies that the opening of the N-domain hydrophobic cleft is the primary conformational change leading toward activation of muscle contraction. That this Ca^{2+}-induced opening

† Supported by National Institutes of Health Grant AR21673.

* Corresponding author. Address: Boston Biomedical Research Institute, 64 Grove Street, Watertown, MA 02472. Telephone: 617-658-7807. Fax: 617-972-1753. E-mail: tao@bbri.org.

‡ Boston Biomedical Research Institute.

§ Massachusetts General Hospital.

|| Department of Biological Chemistry and Molecular Pharmacology, Harvard Medical School.

⊥ Department of Neurology, Harvard Medical School

Department of Biochemistry, Tufts University School of Medicine.

[1] Abbreviations: Tn and Tm, rabbit skeletal troponin and tropomyosin, respectively; TnC, TnI, and TnT, the Ca^{2+}-binding, inhibitory, and Tm-binding subunits of Tn; S1, myosin subfragment 1; TnI121, TnI104, and TnI133, TnI mutants with single cysteines at positions 121, 104, and 133, respectively; TnC12, TnC48, TnC82, and TnC125, TnC mutants with single cysteines at positions 12, 48, 82, and 125, respectively; TnC98, native TnC; TnI_{96-116}, fragment corresponding to residues 96−116 of TnI; BP−IA, benzophenon-4-iodoacetamide; BP, the benzophenone moiety; $TnC48^{BP}$ and $TnC82^{BP}$, BP-labeled TnC48 and TnC82, respectively; DTT, dithiothreitol; EDTA, ethylenediamine-tetraacetic acid; HEPES, N-(2-hydroxyethyl) piperazine-N′-(2-ethanesulfonic acid); Nbs_2, 5,5′-dithio-bis-2-nitrobenzoic acid; SDS-PAGE, sodium dodecyl sulfate polyacrylamide gel electrophoresis; FRET, Förster resonance energy transfer.

10.1021/bi020396m CCC: $22.00
Published on Web 09/27/2002

of TnC's N-domain cleft is functionally significant was demonstrated by site-directed-mutagenesis studies (*11*, *12*). This scenario was proposed by Herzberg et al. (*13*) prior to the availability of the $4Ca^{2+}$•TnC structure based on sequence and structural similarity between the N- and C-domains; these authors also proposed that the open N-domain cleft may provide an additional binding site for some segment of TnI, thereby providing a mechanism for the transmission of the regulatory signal from TnC to TnI.

TnI has long been known to be capable of binding actin and inhibiting actomyosin ATPase activity by itself (*14*). Early studies showed that a cyanogen bromide fragment, TnI_{96-116} (*15*), or peptides related to this TnI fragment (*16*) can mimic such properties of intact TnI as TnC and actin binding, and inhibiting actomyosin ATPase activity. A more recent study showed that the synthetic peptide TnI_{96-148} has an higher inhibitory activity than TnI_{96-139}, implicating residues 140−148 as a "second actin-binding site". Our photo-cross-linking studies on the complete Tn•Tm•F-actin synthetic thin filament showed that the benzophenone (BP) moiety attached at TnI residues 104 or 133 in the inhibitory and near the second actin binding region, respectively, photo-cross-linked to actin in the absence but not in the presence of Ca^{2+} (*17*, *18*), demonstrating that these two regions do indeed undergo Ca^{2+}-dependent translocation to actin. Very recently we showed that the site of photo-cross-linking in actin for both $TnI104^{BP}$ and $TnI133^{BP}$ is Met47 in the so-called DNase-binding loop of actin (*19*).

Extensive studies on the interactions between TnC and TnI were carried out using fragments or peptides derived from both subunits. A variety of studies showed that the two proteins interact with each other in an antiparallel manner (*20*−*25*). In particular, TnI_{1-40} was shown to in teract with TnC's C-domain (*25*, *26*), and the crystal structure of TnC complexed with TnI_{1-47} revealed that the peptide is bound at TnC's C-domain hydrophobic cleft as an α-helix (*27*). Using C-terminal TnI peptides of different lengths, it was deduced that TnI residues 116−131, termed as the "second TnC-binding region", interact with the N-domain of TnC. Our FRET study showed that TnI residue 117 is located near the B- and C-helices in the N-domain of TnC (*28*), consistent with the above notion. Extensive NMR studies show that peptides related to this region are bound at TnC's N-domain cleft (*29*−*32*).

Our series of photo-cross-linking studies on the intact Tn complex showed that BP-labeled TnC12 photo-cross-links to TnI residues 132−141 (*33*), TnC21 to TnI residues 96−134 (*34*), TnC48 and TnC82 to TnI residue 121 (*35*), TnC57 to TnI residues 113−121 (*36*), TnC89 to TnI residues 108−113 (*33*), native TnC (which has a single cysteine at position 98) to TnI residues 103−111 (*37*), TnC158 to TnI residue 21 (*34*), and TnI6 to TnC residue 133 (*38*). These results are generally in support of the antiparallel interaction between TnI and TnC. Additionally, BP-labeled TnI48, TnI64, and TnI89 were found to photo-cross-link with TnT (*18*). Taking into consideration all the available information on the interactions between the Tn subunits, we have proposed a structural and functional model for TnI and TnC in the ternary Tn complex (*18*) (Figure 7). A key feature of this model is that the TnI region that contains Met121 (residues 114−125, termed here as the triggering region) is bound at TnC's N-domain hydrophobic cleft in the presence of Ca^{2+}. This is based on molecular modeling (*27*), binding (*26*), and NMR (*29*−*32*) studies, and particularly on our photo-cross-linking study showing that in the intact Tn complex the BP-label attached at TnC residue 48 or 82 at opposite sides of the N-domain hydrophobic cleft photo-cross-links to TnI Met121 (*35*).

Recently the crystal structure of the complex between cardiac TnC, a fragment of TnI lacking the first 33 residues, and a C-terminal fragment of TnT has been reported in preliminary form (*39*). Although the coordinates of this structure are not yet available, a visual comparison between this structure and the model in Luo et al. (*18*) reveals several similar features. For example, in both structures TnI's N-terminal helix is bound at TnC's C-domain hydrophobic cleft; a hairpin turn is found at residues 50−53 (rabbit skeletal numbering), followed by a region that forms a coiled coil with TnT; more importantly, the corresponding triggering region in cardiac TnI can be seen to be bound at TnC's N-domain hydrophobic pocket (Takeda, S., and Maeda, Y. (2002) personal communication), in excellent agreement with the previous studies discussed above. The major difference between the two models is that in the crystal structure the TnI-TnT coiled coil region extends from the hairpin turn to the equivalent of skeletal TnI's residue 104, whereas in the Luo et al. model (*18*), this region extends only to residue 89. Clearly, much more will be learned from this crystal structure once the coordinates are available.

Thus, at present the evidence for TnI's triggering region being bound at TnC's N-domain cleft in the presence of Ca^{2+} is relatively strong. However, the events that occur upon the closure of TnC's N-domain cleft in response to Ca^{2+}-removal are still unclear, as is the mechanism whereby the Ca^{2+}-regulatory signal is transmitted from TnC to TnI. The present study is designed to address these questions. We first examined the effect of photo-cross-linking between TnC residues 48 or 82 and TnI residue 121 on the inhibitory activity of Tn. We then constructed a mutant TnI with a single Cys at position 121 (TnI121) and studied the propensity for disulfide cross-linking between TnI121 and TnC mutants with single cysteines at various sites. Finally, we analyzed how the regulatory activity of Tn is affected by the Met-to-Cys mutation in TnI121 and by disulfide cross-linking between TnI121 and TnC48 or TnC82. Our results further demonstrate that TnI residue 121 interacts with TnC's N-domain hydrophobic cleft in the presence of Ca^{2+} and that both photo- and disulfide cross-linking abolished TnI's inhibitory activity in the absence of Ca^{2+}. These present and previous findings suggest a simple mechanism for the Ca^{2+}-dependent inhibitory function of TnI.

EXPERIMENTAL PROCEDURES

Chemicals. Unless specified otherwise, common reagents and buffer components were from Sigma. HEPES was from Research Organics (Cleveland, OH), and BP−IA and dansylaziridine were from Molecular Probes (Eugene, OR). Materials for recombinant DNA procedures were from Life Technologies. Materials for gel electrophoresis were from Bio-Rad (Hercule, CA).

Protein Preparation and Modification. Wild-type TnI, TnC, TnT, Tm, and actin were purified from rabbit skeletal muscle according to established methods (*40*, *41*). Rabbit

skeletal myosin was prepared as described previously (*42*) and stored in 50% glycerol at −20 °C. Chymotryptic S1 was prepared from purified myosin according to (*43*). The S1 was further purified on a Sephadex G-75 gel-filtration column and stored at −80 °C with 4 mg of sucrose added per mg of S1. The cDNA constructs for TnI121, TnC48, and TnC82 were prepared by the PCR mutagenesis method of overlap extension (*44*). The mutant proteins were expressed in *E. coli* and purified as described previously (*35*, *45*).

The engineered cysteines in TnC48 and TnC82 were labeled with BP−IA using a previously described procedure (*35*). Labeling of native TnC with dansylaziridine at Met25 followed a procedure based on ref *46* modified by ref *47*. TnC Cys98 was first blocked by incubating the freshly reduced TnC (∼50 μM) with 10-fold excess Nbs_2 in a solution containing 10 mM HEPES, pH 7.5, 0.1 M NaCl, 2 mM EDTA, for 30 min at room temperature, followed by incubation for 2 h at 4 °C. After extensive dialysis in a solution containing 10 mM HEPES, pH7.5, 0.1 M NaCl, and 0.2 mM $CaCl_2$, dansylaziridine from a freshly prepared stock in ethanol was added to TnC in 2-fold molar excess. Following incubation for 24 h at 15 °C, excess probe was removed by dialysis in the above Ca^{2+}-containing solution. Typical efficiency of the incorporation was ∼50%. Reconstitution of the Tn and thin filament complexes were carried out as described previously (*35*). The samples containing BP-labeled TnC's were kept in darkness prior to experimentation.

The concentration of TnC after BP−IA or dansylaziridine labeling was determined using a bicinchoninic acid-based protein assay kit (BCA) from Pierce (Rockford, IL). Other concentrations were determined spectrophotometrically using the following specific absorbances or extinction coefficients: $E_{280} = 0.18$, 0.4, 0.50, 1.09, and 0.77 $(mg/mL)^{-1}$ cm^{-1} for TnC, TnI, TnT, actin, and myosin S1, respectively; $E_{277} = 0.24$ $(mg/mL)^{-1}$ cm^{-1} for Tm; $\epsilon_{331} = 4120$ M^{-1} cm^{-1}, $\epsilon_{280} = 1250$ M^{-1} cm^{-1} for dansylaziridine, and $\epsilon_{280} = 13000$ M^{-1} cm^{-1} for the BP moiety.

Photo- and Disulfide Cross-Linking. The reconstituted ternary Tn complex containing $TnC48^{BP}$ or $TnC82^{BP}$ was exposed to UV irradiation to elicit photo-cross-linking between the BP moiety and Met121 of TnI as described (*35*). Disulfide cross-linking by air oxidation between the engineered cysteine in TnI121 and those in the various single cysteine mutants of TnC was allowed to occur under nonreducing conditions as follows: ternary Tn complexes containing TnI121 and the desired TnC mutant were first freshly reconstituted in the presence of DTT and then dialyzed for 20 h (with one change of fresh buffer after the first 4 h) against DTT-free buffers containing 10 mM HEPES, pH 7.5, 0.1 M NaCl, and 0.2 mM $CaCl_2$ or 2 mM EGTA and 6 mM $MgCl_2$ for cross-linking in the presence or the absence of Ca^{2+}, respectively. Tn samples containing increasing extents of disulfide cross-linking between TnI121 and TnC48 or TnC82 were prepared by the addition of increasing amounts of Nbs_2 following dialysis for 2−3 h against DTT-free buffer containing 0.2 mM $CaCl_2$. The extents of cross-linking were monitored with SDS-PAGE.

SDS-PAGE and Densitometry. SDS gels containing 12.5% acrylamide were used to resolve TnC, TnI, TnT, and the cross-linked components. The gels were stained with Coomassie Blue and digitized using a UMAX SuperVista S-12 scanner and the Adobe Photoshop software. Densitometric analysis was carried out using the NIH Image software. Its Gel Plotting Macros tool was first used to plot the intensity versus the vertical dimension of a gel, so that the bands in an individual lane were depicted as a series of peaks. The Wand Tool was then used to integrate the area under a peak of interest, which was then used as a relative measure of the quantity in a protein band.

ATPase Activity Measurements. Ternary Tn complexes containing unmodified or BP-labeled subunits were first reconstituted, followed by photo- or disulfide cross-linking prior to the ATPase assay as described above. At the time of assay, the Tn's were added to the previously reconstituted S1·Tm·F-actin complex with final concentrations of 0.6 μM Tm, 3 μM actin, and 1.5 μM S1. The Tn concentration was either 0.6 μM or as shown in the figures. The assay buffer contained 20 mM Tris, pH 8.0, 5 mM $MgCl_2$, 20 mM NaCl, and either 0.5 mM $CaCl_2$ or 0.5 mM EGTA for the activated or the inhibited activity, respectively. The ATPase reactions were initiated by the addition of ATP (final concentration 1 mM) after 10 min incubation at 25 °C. Photometric determination of the inorganic phosphate released in a time course of 8 min (with $CaCl_2$) or 20−30 min (with EGTA) was carried out as described previously (*45*).

Fluorescence Titration. The fluorescence of dansylaziridine attached to Met25 of TnC is known to be higher in the presence of Ca^{2+} than in its absence (*46*, *47*). It is decreased by the binding of TnI in the presence of Ca^{2+} but increased in the absence of Ca^{2+} (*46*, *47*). These changes were used to measure the affinity of TnI or TnI121 for TnC. Solutions of TnC containing 0.05 or 0.5 μM labeled fluorophore (0.094 or 0.94 μM TnC, respectively) were prepared for binding in the presence of 0.2 mM $CaCl_2$ or 0.5 mM EGTA and 5 mM $MgCl_2$, respectively. Other components of the assay buffer were 10 mM HEPES, pH 7.5, and 0.1 M NaCl. The stock solution of wild-type TnI or TnI121 (102 μM and 94 μM, respectively, in 10 mM HEPES, pH7.5, 0.5 M NaCl) was titrated manually into 600 μl TnC solution in 1 μl increments until little change could be induced by further additions (typically 15−20). The steady-state fluorescence was measured at room temperature with a Perkin-Elmer spectrofluorometer. A binding isotherm was obtained by plotting the relative change in fluorescence versus TnI concentration after appropriate corrections for dilution. Using a nonlinear fitting tool provided in the graphing software KaleidaGraph, the data were fit to a 1:1 binding model to obtain the association constant K_a:

$$\frac{\Delta F}{\Delta F_{max}} = \frac{([TnI]_n + [TnC]_0 + K_D) - \sqrt{([TnI]_n + [TnC]_0 + K_D)^2 - 4[TnI]_n[TnC]_0}}{2[TnC]_0}$$

where ΔF is the absolute value of the total change in fluorescence after the nth TnI addition, ΔF_{max} is the absolute value of the maximum change at the end of the titration, K_D is the reciprocal of the association constant K_a, $[TnC]_0$ is the initial concentration of the dansylaziridine-labeled TnC, and $[TnI]_n$ is the total concentration of TnI or TnI121 after the *n*th addition and is the independent variable in the equation.

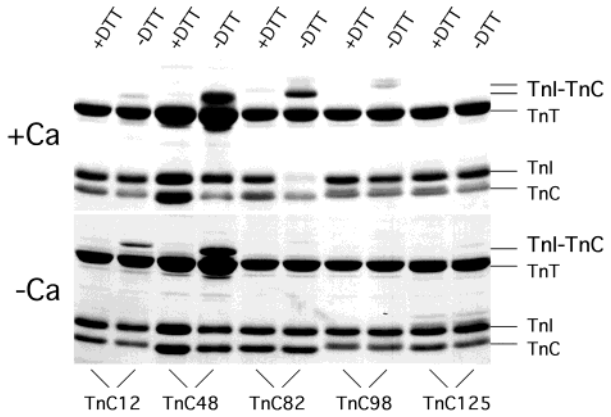

FIGURE 1: Disulfide cross-linking between TnI121 and single cysteine TnC mutants in the presence (top panel) and absence (bottom panel) of Ca^{2+}. Ternary Tn complexes containing TnI121 and the appropriate TnC mutant were allowed to oxidize in air (see Methods). The control samples for each TnC mutant were treated with 10 mM DTT (+DTT) prior to SDS-PAGE.

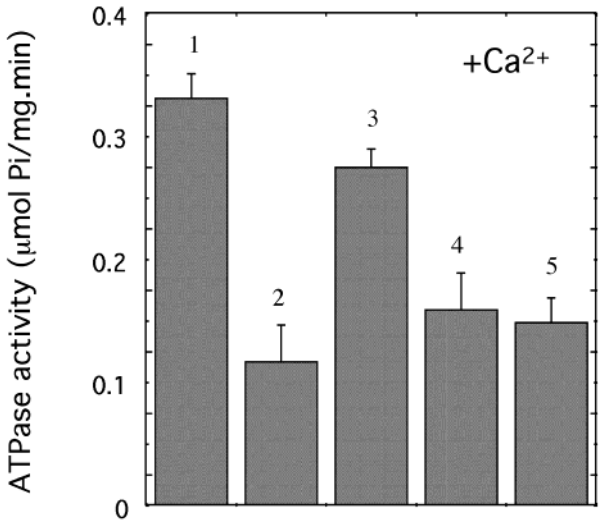

FIGURE 2: Impaired activation of acto-S1 ATPase activity in the presence of Ca^{2+} by Tn containing TnI121. Column 1, S1·A; column 2, S1·Tm·A; column 3, S1·C·I·T·Tm·A; column 4, S1·C·I121·T·Tm·A; and column 5, S1·C48·I121·T·Tm·A, where A is F-actin. C, I, and T are native TnC, TnI, and TnC, respectively; I121 and C48 are TnI121 and TnC48, respectively. For the ATPase measurements, [S1] = 1.5 μM, [actin] = 3.0 μM, [Tm] = [Tn] = 0.6 μM in a solution containing 20 mM Tris, pH 8.0, 5 mM $MgCl_2$, 20 mM NaCl, and 0.5 mM $CaCl_2$.

RESULTS

The Effect of Photo-Cross-Linking between TnC48 or TnC82 and TnI121 on the Ca^{2+}-Absent Inhibition of Regulated Acto-S1 ATPase. Previously we have shown, both $TnC48^{BP}$ and $TnC82^{BP}$ photo-cross-linked to Met121 of TnI in the presence of Ca^{2+} (*35*). Here we examine the effect of this cross-linking on the Ca^{2+}-absent inhibitory activity of Tn. The ternary $TnC48^{BP}$·TnI·TnT or $TnC82^{BP}$·TnI·TnT complex was UV irradiated in the presence of Ca^{2+} for 0−30 min as described in (*35*), and the relative extent of photo-cross-linking was monitored by densitometry of the TnC-TnI bands on SDS-PAGE. The same irradiated samples were combined with S1·Tm·F-actin, and the S1·Tn·Tm·F-actin ATPase activity was assayed in the absence of Ca^{2+}. We found that both the extent of cross-linking and the ATPase activity increased (inhibitory activity decrease) with time of radiation, both saturating at ~10 min of radiation (data not shown). This suggests that a photo-cross-link between TnC residue 48 or 82 and TnI residue 121 impairs the inhibitory activity of Tn. However, the actual photo-cross-linking yield was too low to be measured reliably, so that a quantitative correlation could not be established using this approach.

Disulfide Cross-Linking between TnI121 and TnC Mutants. To examine the effects of cross-linking between TnI and TnC quantitatively we constructed the single cysteine mutant TnI121 for disulfide cross-linking experiments. To verify that TnI residue 121 is indeed in TnC's N-domain hydrophobic cleft, disulfide cross-linking experiments were carried out using Tn reconstituted with native TnT, TnI121, and the single-cysteine TnC mutants TnC12, TnC48, TnC82, TnC98, and TnC125. The results show that in the presence of Ca^{2+}, only small amounts of disulfide cross-linking to TnI121 was observed for TnC12 and TnC98, and none at all for TnC125 (Figure 1, top panel). Extensive disulfide cross-linking was only observed for TnC48 and TnC82. In the absence of Ca^{2+}, only TnC48 exhibited appreciable disulfide cross-linking with TnI121 (Figure 1, bottom panel). Interestingly, an increase in disulfide cross-linking was observed for TnC12.

Impaired Ca^{2+} Activation of S1·Tm·F-Actin ATPase by Tn Containing TnI121. We investigated the effect of the Met-to-Cys mutation in TnI121 on the activation of S1·Tn·Tm·F-actin ATPase activity by Ca^{2+}. At the ratio of S1:actin used in the assays, Tm inhibits the ATPase activity of S1·F-actin (Figure 2, column 2 vs 1). The addition of reconstituted Tn containing all native subunits in the presence of Ca^{2+} almost fully reversed the inhibition (column 3). This activation effect is impaired when Tn containing TnI121 and native TnC or TnC48 was used in the assays (columns 4 and 5). This is in contrast to the normal regulatory function of other single Cys mutants of TnI, e.g., TnI6, TnI48, TnI89, TnI104, and TnI133, etc. (*18*).

Binding of TnI121 to Fluorescently Labeled TnC. To test if the Met-to-Cys mutation at residue 121 weakens the binding of TnI121 to TnC, which could account for the observed impairment of the activation process, the association constant between TnI121 and TnC was measured by fluorescence titration. TnC was first labeled at Met25 with the fluorescence probe dansylaziridine, and the binding of TnI121 or that of native TnI was monitored by the probe fluorescence. It is known that this fluorescence is sensitive to both Ca^{2+} and TnI binding, being 10-fold higher in the presence than in the absence of Ca^{2+}, and TnI binding induces a 50% decrease or 100% increase in the presence or absence of Ca^{2+}, respectively (*11*). As shown in Figure 3, the titration curves for the binding of TnI121 to dansylaziridine-labeled TnC differ very little from that of control TnI both in the presence (Figure 3A) and in the absence (Figure 3B) of Ca^{2+}. When the curves were fit with a binding isotherm, we obtained the following association constants: in the presence of Ca^{2+}, $K_a = (1.2\pm0.1) \times 10^7$ and $(1.3\pm0.1) \times 10^7$ M^{-1} for native TnI and TnI121, respectively; in the absence of Ca^{2+}, $K_a = (2.3\pm0.3) \times 10^6$ and $(1.7 \pm0.3) \times 10^6$ M^{-1} for native TnI and TnI121, respectively. It can be seen that the association constants for native TnI and TnI121 are very similar to each other both in the presence and absence of Ca^{2+}.

The Effects of Disulfide Cross-Linking between TnI121 and TnC48 or TnC82 on the Ca^{2+}-Absent Inhibition of Acto-S1

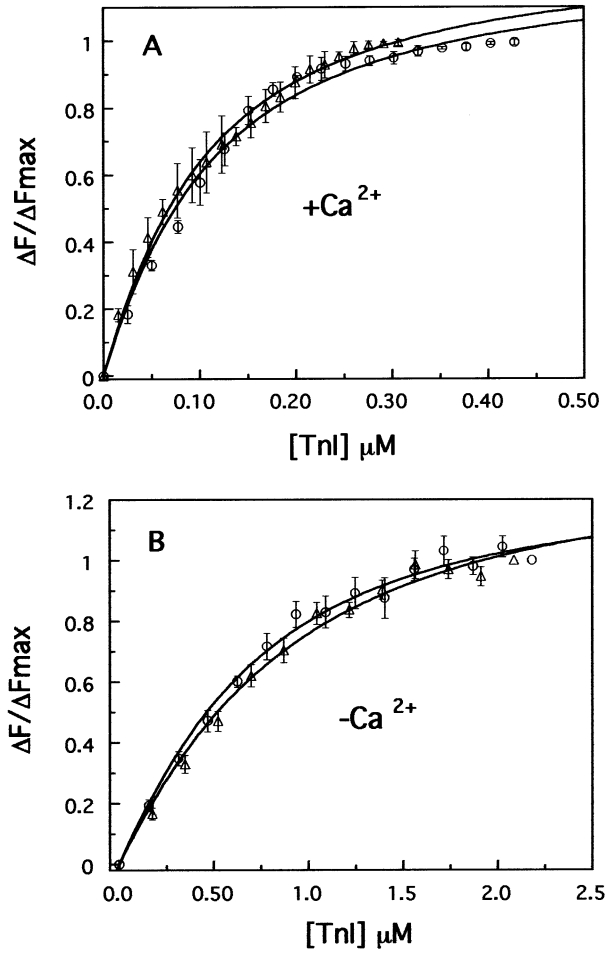

FIGURE 3: Fluorescence titration of dansylaziridine-labeled TnC by native TnI (Δ) and TnI121 (o) in the presence (panel A) and absence (panel B) of Ca^{2+}. Solid lines are best fits obtained by nonlinear regression assuming a 1:1 binding stoichiometry between the proteins. See text for values of the association constant.

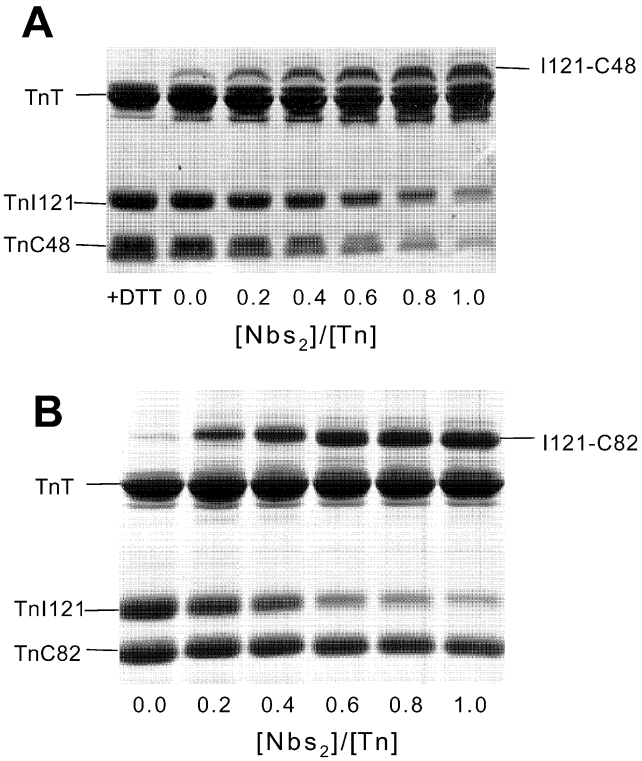

FIGURE 4: Nbs_2-induced disulfide cross-linking of TnI121 with TnC48 (panel A) or TnC82 (panel B) in the presence of Ca^{2+}. Increasing amounts of Nbs_2 were added to Tn (~30 μM) reconstituted with TnI121, TnC48, or TnC82 and native TnT to induce efficient disulfide cross-linking. The amount of TnC82 in panel B was in excess over TnI121.

ATPase. To investigate whether disulfide cross-linking between TnI121 and TnC48 or TnC82 impairs the inhibitory activity of Tn in the absence of Ca^{2+}, we treated Tn containing TnI121 and TnC48 or TnC82 with increasing amounts of Nbs_2 to promote the disulfide cross-linking reaction (panels A or B, respectively, of Figure 4). Samples of Tn containing increasing amounts of cross-linking were titrated into S1·Tm·F-actin and the ATPase activity measured in the absence of Ca^{2+}. As shown in Figure 5A, the resultant inhibition curve of DTT-treated TnC48·TnI121·TnT is nearly the same as that of Tn containing all native subunits (C·I·T in Figure 5A), indicating that neither the Gln to Cys mutation in TnC48 nor the Met-to-Cys mutation in TnI121 impaired the inhibitory function of Tn**.** As the molar ratio of Nbs_2 to TnC48·TnI121·TnT or TnC82·TnI121·TnT was increased, both the extent of cross-linking (Figure 4A,B) and the ATPase activity (Figure 5A,B) increased, indicating a progressive loss in the Tn's inhibitory function. The percent of TnI121 disulfide cross-linked to TnC48 or TnC82 at each Nbs_2 to Tn ratio was determined by quantitative densitometry of the gel shown in panels A and B, respectively of Figure 4. When the ATPase activities at Tn:Tm = 1.25:1 was plotted against the percent TnI disulfide cross-linking, a linear correlation was obtained in both cases (Figure 6A,B). Because TnI121 has a higher tendency to disulfide cross-link with TnC48, treatment of DTT was necessary to achieve 0% cross-linking.

DISCUSSION

To aid in the interpretation of our disulfide cross-linking results, we may refer to the structural model for TnC and TnI in the Tn complex proposed by Luo et al. (*18*) (Figure 7). The table in the inset shows the calculated distances between TnI residue 121 and the TnC residues involved. In the presence of Ca^{2+}, we observed little or no disulfide cross-linking between TnI121 and TnC98 or TnC125; this is most likely because TnI residue 121 is relatively far from these TnC residues, as the model indicates. Very little TnI121-TnC12 cross-linking was observed even though the predicted distance between the two residues involved is relatively small. Inspection of the space-filled model reveals, however, that with the triggering region (TnI residues 114−125) bound at TnC's N-domain cleft, TnI residue 121 is obstructed by residues on TnC's A-helix from disulfide cross-linking with TnC residue 12, accounting for the low cross-linking yield. In contrast TnC residues 48 and 82 are both proximal and accessible for efficient TnI121-TnC48 and TnI121-TnC82 disulfide cross-linking to take place.

In the absence of Ca^{2+}, according to the model, the triggering region moves out of TnC's N-domain cleft but remains in the vicinity of TnC. TnI residue 121 is still too far from TnC residues 98 and 125 for TnI121-TnC98 and TnI121-TnC125 disulfide cross-linking to occur. Although TnI residue 121 is still close to both TnC residues 48 and 82, the latter is now shielded from disulfide cross-linking

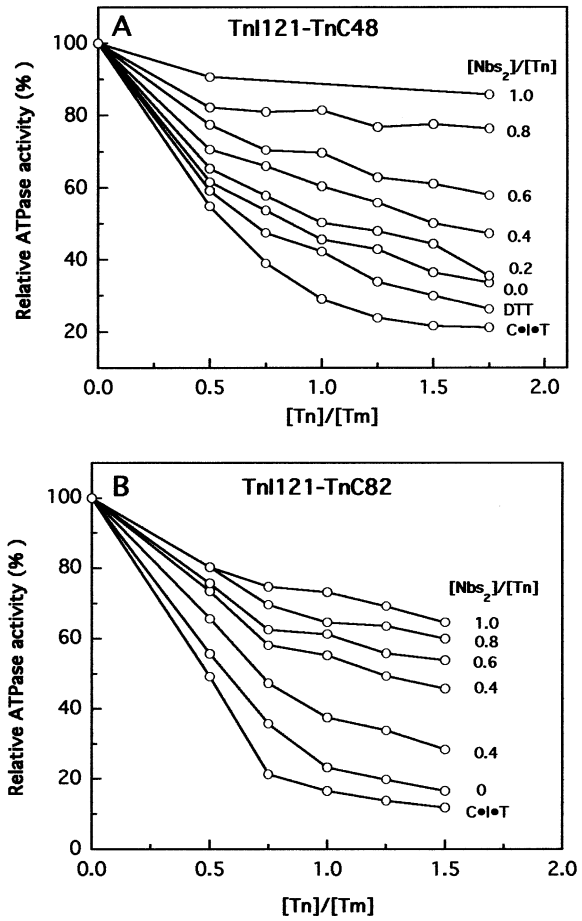

FIGURE 5: Ca^{2+}-free ATPase activities of S1·Tm·F-act in the presence of Tn containing disulfide cross-linked TnI121-TnC48 (panel A) or TnI121-TnC82 (panel B). Samples of Tn containing increasing amounts of TnI-TnC disulfide cross-linking (Figure 4) were titrated into S1·Tm·F-actin in the same buffer as that in Figure 2, except that 0.5 mM EGTA replaces 0.5 mM $CaCl_2$. ATPase activity is plotted as the percent of that for S1·Tm·F-actin. A progressive loss in the inhibitory activity (increase in ATPase activity) with extent of disulfide cross-linking can be seen.

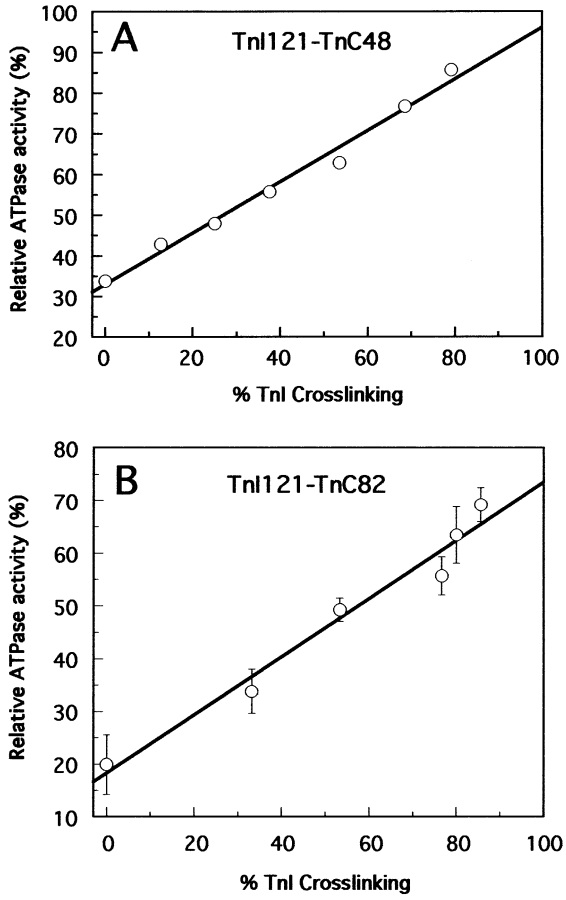

FIGURE 6: Correlation between the loss of inhibitory activity and the extent of TnI121-TnC48 (panel A) or TnI121-TnC82 (panel B) disulfide cross-linking. The Ca^{2+}-free ATPase activities of S1·Tn·Tm·F-actin at a Tn:Tm molar ratio of 1.25 (Figure 5) were plotted against the percent of TnI engaged in cross-linking, calculated as $(1 - I_i/I_o) \times 100$, where I_o and I_i are the intensities of the TnI121 band prior to and at the ith addition of Nbs_2, respectively.

by residues in TnC's linker region between helices B and C (see Figure 7). On the other hand, TnC residue 48 is exposed and can still undergo efficient disulfide cross-linking to TnI residue 121, as was observed. Curiously, there was an increase in the TnI121-TnC12 disulfide cross-linking yield. This may be because the triggering region is now relatively mobile, so that TnI residue 121 is capable of "reaching" TnC residue 12 under the Ca^{2+}-absent condition. Thus, our disulfide cross-linking results are consistent with the scenario that in the presence of Ca^{2+} TnI residue 121 and the triggering region are in TnC's N-domain cleft, as well as with other features of the model of Luo et al. (*18*).

We found that Tn containing TnI121 is incapable of fully activating S1·Tn·Tm·F-actin ATPase activity (Figure 2) although the overall affinity of TnI121 to TnC is not different from that of the wild-type TnI (Figure 3), so that the impairment cannot be attributed to partial dissociation of the Tn complex. In our previous studies we have shown that all our single cysteine TnI mutants that lack the three endogenous cysteines in TnI (Cys48, Cys64, and Cys133) exhibit normal regulatory activity (*18*) [see also ref *48*]. Therefore, the adverse effect observed in this work is attributable to the Met-to-Cys mutation at TnI residue 121, a mutation that would considerably reduce the hydrophobicity of this residue. Inspection of this region of TnI and TnC in the Luo et al. model [which was derived from a molecular modeling study by Vassylyev et al., *27*] reveals that TnI Met121 is engaged in extensive hydrophobic interaction with residues in TnC's N-domain hydrophobic cleft (as was specifically pointed out by Vassylyev et al., *27*). This mutation can therefore be expected to reduce the interaction between the triggering region and TnC's N-domain cleft. The underlying mechanism of how this leads to impairment of Tn's Ca^{2+}-activation activity will be discussed later in this section in the context of the overall model for Tn regulation.

In this work we found that when $TnC48^{BP}$ or $TnC82^{BP}$ was photo-cross-linked to TnI residue 121 the ability of Tn to inhibit S1·Tm·F-actin ATPase activity in the absence of Ca^{2+} was progressively lost as the extent of photo-cross-linking increased. Similarly, when TnC48 or TnC82 was disulfide cross-linked to TnI121, the loss of inhibitory activity was correlated with the extent of disulfide cross-linking. Since both the photo- and the disulfide cross-linking were carried out in the presence of Ca^{2+}, we can expect TnI's triggering region to be tethered within TnC's N-domain cleft and will remain so even after removal of Ca^{2+}. These results therefore indicate that if the triggering region does not vacate

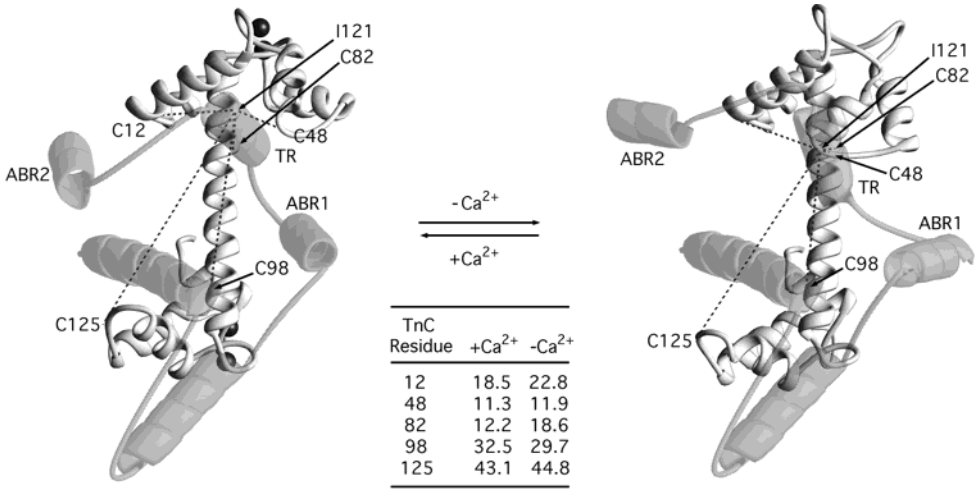

TnC Residue	+Ca^{2+}	-Ca^{2+}
12	18.5	22.8
48	11.3	11.9
82	12.2	18.6
98	32.5	29.7
125	43.1	44.8

FIGURE 7: Proposed structure of TnC and TnI in the Tn complex, adapted from the model of Luo et al. (*18*). Labeled are residues involved in the disulfide cross-linking experiments: I121 is TnI residue 121; C12, C48, C82, C98, C125 are TnC residues 12, 48, 82, 98, 125, respectively. Depicted in solid contour is TnC; in light contour is TnI. Regions of TnI depicted as helices correspond to α-helical segments predicted by sequence analysis. ABR1 and ABR2 correspond to TnI's actin-binding regions 1 and 2, respectively (residues 89−113 and 130−150, respectively); TR corresponds to TnI's triggering region (residues 114−124). This region is located within TnC's open N-domain hydrophobic cleft when Ca^{2+} is present. In the absence of Ca^{2+}, it moves out of the closed cleft to the front of TnC. Inset: calculated distances (in Å) between TnI residue 121 and the TnC residues in the presence and absence of Ca^{2+}.

TnC's N-domain cleft upon Ca^{2+} removal, subsequent events in the inhibition process cannot occur.

We reported earlier that in the synthetic Tn·Tm·F-actin filament BP attached at residues 104 and 133 in the first and second actin-binding regions of TnI, respectively, photo-cross-linked to TnC but not to actin in the presence of Ca^{2+} (*18*); in the absence of Ca^{2+}, they photo-cross-linked to actin but not to TnC. In contrast, BP attached at TnI residue 121 photo-cross-linked only to TnC and not to actin in both the presence and the absence of Ca^{2+} (*18*). Taking together the previous work and the present study, we believe all the results suggest a simple mechanism for the role of TnI in thin filament regulation: of the various TnI segments, the first and second actin binding regions possess residues that interact strongly with actin but weakly with TnC. Residues in TnI's triggering region, on the other hand, interact strongly with residues in TnC's N-domain hydrophobic cleft when it is open, and not with those of actin. When Ca^{2+} is present and bound at TnC's N-domain sites, TnI's triggering region is tightly held in the open N-domain cleft of TnC, which serves to restrain the flanking first and second actin-binding regions close to TnC and away from actin (see Figure 7). When Ca^{2+} is removed, the triggering region vacates the closed N-domain cleft of TnC. Without the strong interaction between the triggering region and TnC, the two actin-binding regions are free to engage in strong interaction with actin, initiating further events in regulation. While the movements of the actin-binding regions toward actin during the inhibition process may cause the triggering region of TnI to move slightly away from TnC, it remains in the vicinity of TnC so that it can readily interact with TnC's open N-domain hydrophobic cleft when Ca^{2+} is present again.

This model is in excellent agreement with our observations here. When the triggering region is tethered to TnC via photo- or disulfide cross-linking between TnI residue 121 and TnC residue 48 or 82, TnI's actin-binding regions remain constrained from interacting with actin even in the absence of Ca^{2+}, resulting in impaired inhibition as was observed in this work. Conversely, when the interaction between the triggering region and TnC's N-domain pocket is weakened by the Met-to-Cys mutation at TnI residue 121, the ability of the triggering region to constrain the actin-binding regions from interacting with actin would be compromised, thereby giving rise to the impaired Ca^{2+}-activation, as was also observed in this work. Recently we reported that TnI's actin-binding regions interact with Met47 in the outer domain of actin (*19*). Image reconstruction studies showed that some portion of Tn interacts with actin's outer domain (*49*, *50*). This, together with the observation that Tm is located at actin's outer domain in the inhibited state (*50*, *51*), has led to the proposal that when Ca^{2+} is absent the actin-binding regions of TnI interact with Tm at actin's outer domain, thereby stabilizing Tm at it's inhibitory position (*19*, *49*, *52*). This proposal, together with the one above, may provide the framework for a complete description of the Ca^{2+}-regulatory process in striated muscle. Clearly, much additional work will be required to test the validity of these hypotheses. Site-directed-mutagenesis experiments toward that end are underway in our laboratory.

ACKNOWLEDGMENT

We thank Dr. Z. Grabarek for helpful discussions and Dr. K. Langsetmo for assistance in the preparation of this manuscript.

REFERENCES

1. Gordon, A. M., Homsher, E., and Regnier, M. (2000) *Physiol. Rev. 80*, 853−924.
2. Zot, A. S., and Potter, J. D. (1987) *Annu. Rev. Biophys. Biophys. Chem. 16*, 535−559.
3. Leavis, P. C., and Gergely, J. (1984) *CRC Crit. Rev. Biochem. 16*, 235−305.
4. Grabarek, Z., Tao, T., and Gergely, J. (1992) *J. Muscle Res. Cell Motil. 13*, 383−393.
5. Herzberg, O., and James, M. N. G. (1985) *Nature 313*, 653−659.
6. Houdusse, A., Love, M. L., Dominguez, R., Grabarek, Z., and Cohen, C. (1997) *Structure 5*, 1695−1711.
7. Sundaralingam, M., Bergstrom, R., Strasburg, G., Rao, S. T., Greaser, M., and Wang, B. C. (1985) *Science 227*, 945−948.

8. Soman, J., Tao, T., and Phillips, G. N. (1999) *Proteins 37*, 510−511.
9. Sheng, Z., Strauss, W. L., Francois, J. M., and Potter, J. D. (1990) *J. Biol. Chem. 265*, 21554−21560.
10. Johnson, J. D., Charlton, S. C., and Potter, J. D. (1979) *J. Biol. Chem. 254*, 3497−3502.
11. Grabarek, Z., Tan, R.-Y., Wang, J., Tao, T., and Gergely, J. (1990) *Nature 345*, 132−135.
12. Fujimori, K., Sorenson, M., Herzberg, O., Moult, J., and Reinach, F. C. (1990) *Nature 345*, 182−184
13. Herzberg, O., Moult, J., and James, M. N. G. (1986) *J. Biol. Chem. 261*, 2638−2644.
14. Perry, S. V., Cole, H. A., Head, J. F., and Wilson, F. J. (1972) *Cold Spring Harbor Symp. Quantum Biol. 37*, 251−262,
15. Syska, H., Wilkinson, J. M., Grand, R. J. A., and Perry, S. V. (1976) *Biochem. J. 153*, 375−387.
16. Talbot, J. A., and Hodges, R. S. (1981) *J. Biol. Chem. 256*, 2798−2802.
17. Tao, T., Gong, B.-J., and Leavis, P. C. (1990) *Science 247*, 1265−1372.
18. Luo, Y., Wu, J. L., Li, B., Langsetmo, K., Gergely, J., and Tao, T. (2000) *J. Mol. Biol. 296*, 899−910.
19. Luo, Y., Leszyk, J., Li, B., Li, Z. X., Gergely, J., and Tao, T. (2002) *J. Mol. Biol. 316*, 429−434.
20. Sheng, Z., Pan, B. S., Miller, T. E., and Potter, J. D. (1992) *J. Biol. Chem. 267*, 25407−25413.
21. Pearlstone, J. R., Sykes, B. D., and Smillie, L. B. (1997) *Biochemistry 36*, 7601−7606.
22. Pearlstone, J. R., and Smillie, L. B. (1995) *Biochemistry 34*, 6932−6940
23. Krudy, G. A., Kleerekoper, Q., Guo, X. D., Howarth, J. W., Solaro, R. J., and Rosevear, P. R. (1994) *J. Biol. Chem. 269*, 23731−23735.
24. Jha, P. K., Mao, C., and Sarkar, S. (1996) *Biochemistry 35*, 11026−11035.
25. Farah, C. S., Miyamoto, C. A., Ramos, C. H. I., da Silva, A. C. R., Quaggio, R. B., Fujimori, K., Smillie, L. B., and Reinach, F. C. (1994) *J. Biol. Chem. 269*, 5230−5240.
26. Tripet, B., Van Eyk, J. E., and Hodges, R. S. (1997) *J. Mol. Biol. 271*, 728−750.
27. Vassylyev, D. G., Takeda, S., Wakatsuki, S., Maeda, K., and Maeda, Y. (1998) *Proc. Natl. Acad. Sci. U.S.A. 95*, 4847−4852.
28. Li, Z., Gergely, J., and Tao, T. (2001) *Biophys. J. 81*, 321−333.
29. McKay, R. T., Tripet, B. P., Hodges, R. S., and Sykes, B. D. (1997) *J. Biol. Chem. 272*, 28494−28500.
30. McKay, R. T., Tripet, B. P., Pearlstone, J. R., Smillie, L. B., and Sykes, B. D. (1999) *Biochemistry 38*, 5478−5489.
31. McKay, R. T., Pearlstone, J. R., Corson, D. C., Gagne, S. M., Smillie, L. B., and Sykes, B. D. (1998) *Biochemistry 37*, 12419−12430.
32. Li, M. X., Spyracopoulos, L., and Sykes, B. D. (1999) *Biochemistry 38*, 8289−8298.
33. Kobayashi, T., Tao, T., Gergely, J., and Collins, J. H. (1994) *J. Biol. Chem. 269*, 5725−5729.
34. Leszyk, J., Tao, T., Nuwaysir, L. M., and Gergely, J. (1998) *J. Muscle Res. Cell Motil. 19*, 479−490.
35. Luo, Y., Leszyk, J., Qian, Y., Gergely, J., and Tao, T. (1999) *Biochemistry 38*, 6678−6688.
36. Kobayashi, T., Tao, T., Grabarek, Z., Gergely, J., and Collins, J. H. (1991) *J. Biol. Chem. 266*, 13746−13751.
37. Leszyk, J., Collins, J. H., Leavis, P. C., and Tao, T. (1988) *Biochemistry 27*, 6983−6987.
38. Luo, Y., Leszyk, J., Li, B., Gergely, J., and Tao, T. (2000) *Biochemistry 39*, 15306−15315.
39. Takeda, S., Yamashida, A., Maeda, K., and Maeda, Y. (2002) *Biophys. J. 82*, 170a.
40. Greaser, M. L., and Gergely, J. (1973) *J. Biol. Chem. 248*, 2125−2133.
41. Spudich, J. A., and Watt, S. (1971) *J. Biol. Chem. 246*, 4866−4871.
42. Wagner, P. D., and Yount, R. G. (1975) *Biochemistry 14*, 1900−1907.
43. Weeds, A. G., and Taylor, R. S. (1975) *Nature 257*, 54−56.
44. Ho, S. N., Hunt, H. D., Horton, R. M., Pullen, J. K., and Pease, L. R. (1989) *Gene 77*, 51−59.
45. Luo, Y., Wu, J.-L., Gergely, J., and Tao, T. (1997) *Biochemistry 36*, 11027−11035.
46. Johnson, J. D., Collins, J. H., and Potter, J. D. (1978) *J. Biol. Chem. 253*, 6451−6458.
47. Grabarek, Z., Grabarek, J., Leavis, P. C., and Gergely, J. (1983) *J. Biol. Chem. 258*, 14098−14102.
48. Kluwe, L., Maeda, K., and Maeda, Y. (1993) *FEBS Lett. 323*, 83−88.
49. Lehman, W., Rosol, M., Tobacman, L. S., and Craig, R. (2001) *J. Mol. Biol. 307*, 739−744.
50. Narita, A., Yasunaga, T., Ishikawa, T., Mayanagi, K., and Wakabayashi, T. (2001) *J. Mol. Biol. 308*, 241−261.
51. Xu, C., Craig, R., Tobacman, L., Horowitz, R., and Lehman, W. (1999) *Biophys. J. 77*, 985−992.
52. Zhou, X., Morris, E. P., and Lehrer, S. S. (2000) *Biochemistry 39*, 1128−1132.

BI020396M